

CONSTRAINTS ON NON-FLAT COSMOLOGIES WITH MASSIVE NEUTRINOS AFTER *PLANCK* 2015YUN CHEN¹, BHARAT RATRA², MAREK BIESIADA^{3,4}, SONG LI⁵, AND ZONG-HONG ZHU³¹ Key Laboratory for Computational Astrophysics, National Astronomical Observatories, Chinese Academy of Sciences, Beijing, 100012, China; chenyun@bao.ac.cn² Department of Physics, Kansas State University, 116 Cardwell Hall, Manhattan, KS 66506, USA³ Department of Astronomy, Beijing Normal University, Beijing 100875, China⁴ Department of Astrophysics and Cosmology, Institute of Physics, University of Silesia, Uniwersytecka 4, 40-007 Katowice, Poland⁵ Department of Physics, Capital Normal University, Beijing 100048, China

Received 2016 March 22; revised 2016 June 29; accepted 2016 July 18; published 2016 September 22

ABSTRACT

We investigate two dark energy cosmological models (i.e., the Λ CDM and ϕ CDM models) with massive neutrinos assuming two different neutrino mass hierarchies in both the spatially flat and non-flat scenarios, where in the ϕ CDM model the scalar field possesses an inverse power-law potential, $V(\phi) \propto \phi^{-\alpha}$ ($\alpha > 0$). Cosmic microwave background data from *Planck* 2015, baryon acoustic oscillation data from 6dFGS, SDSS-MGS, BOSS-LOWZ and BOSS CMASS-DR11, the joint light-curve analysis compilation of SNe Ia apparent magnitude observations, and the *Hubble Space Telescope* H_0 prior, are jointly employed to constrain the model parameters. We first determine constraints assuming three species of degenerate massive neutrinos. In the spatially flat (non-flat) Λ CDM model, the sum of neutrino masses is bounded as $\Sigma m_\nu < 0.165(0.299)$ eV at 95% confidence level (CL). Correspondingly, in the flat (non-flat) ϕ CDM model, we find $\Sigma m_\nu < 0.164(0.301)$ eV at 95% CL. The inclusion of spatial curvature as a free parameter results in a significant broadening of confidence regions for Σm_ν and other parameters. In the scenario where the total neutrino mass is dominated by the heaviest neutrino mass eigenstate, we obtain similar conclusions to those obtained in the degenerate neutrino mass scenario. In addition, the results show that the bounds on Σm_ν based on two different neutrino mass hierarchies have insignificant differences in the spatially flat case for both the Λ CDM and ϕ CDM models; however, the corresponding differences are larger in the non-flat case.

Key words: cosmology: miscellaneous – cosmology: theory – dark energy

1. INTRODUCTION

To date, there is firm evidence for neutrino oscillations (see the reviews of Maltoni et al. 2004; Fogli et al. 2006; Balantekin & Haxton 2013) from measurements on solar (Ahmad et al. 2001), atmospheric (Fukuda et al. 1998), reactor (Ahn et al. 2012; An et al. 2012) and accelerator beam (Agafonova et al. 2010) neutrinos. These measurements imply that neutrinos have small but non-zero masses, with at least two species being non-relativistic today. Experiments have placed restrictive limits on differences of two squared neutrino masses, such as $\Delta m_{21}^2 = m_2^2 - m_1^2 \sim 8 \times 10^{-5} \text{ eV}^2$ (Abe et al. 2008) and $\Delta m_{32}^2 = m_3^2 - m_2^2 \sim 3 \times 10^{-3} \text{ eV}^2$ (Ashie et al. 2005), but give no constraint on their absolute mass scales. Here m_1 , m_2 , and m_3 denote the masses of neutrino mass eigenstates. The measurement of the absolute neutrino mass scale remains a big challenge for both experimental particle physics and observational cosmology. Fortunately, a variety of cosmological probes can provide the crucial complementary information on absolute neutrino mass scale. Current cosmological data can provide an upper limit on the total neutrino mass Σm_ν (summed over the three neutrino families) of order 1 eV or less (Lesgourgues & Pastor 2012), though they are not very sensitive to the neutrino mass hierarchy.

Massive neutrinos are the only particles that have undergone the transition from radiation to matter as the universe expanded and cooled (Lesgourgues & Pastor 2006). Before the non-relativistic transition the neutrinos behave like radiation. Thus, when the total neutrino mass Σm_ν increases, there is more relativistic matter at early times and the matter–radiation equality occurs later, so the scale factor at the epoch of matter–radiation equality a_{eq} increases (i.e., z_{eq} gets lower). The

cosmic microwave background (CMB) radiation and large-scale structure (LSS) distributions are very sensitive to a_{eq} , which provides potential ways to constrain Σm_ν through CMB and LSS observations. In addition, the massive neutrinos are non-relativistic today, so they contribute to the recent expansion rate of the universe as cold dark matter. Moreover, after thermal decoupling the massive neutrinos freely stream a distance called the free-streaming length. This disrupts the structure formation on scales below this length. Because of the above effects, massive neutrinos can leave imprints on cosmological observables. This is why a variety of cosmological tests are sensitive to the absolute scale of neutrino mass, such as the CMB anisotropy, galaxy, and $\text{Ly}\alpha$ forest distributions as well as the distance information from baryon acoustic oscillations (BAOs) and SNe Ia measurements.

The limits on Σm_ν obtained from cosmology, so far, are rather model dependent and vary strongly with the data combination adopted. In Hannestad (2005), it was found that when the dark energy equation of state (EoS) is taken as a free (but constant) parameter, the cosmological bound on Σm_ν is relaxed by more than a factor of two, to $\Sigma m_\nu < 1.48$ eV (95% confidence level; CL), compared with $\Sigma m_\nu < 0.65$ eV (95% CL) in the Λ CDM model. The above results were obtained from a combination of CMB measurements from the first-year *Wilkinson Microwave Anisotropy Probe* (WMAP) observations (Bennett et al. 2003), the galaxy power spectrum based on the Sloan Digital Sky Survey (SDSS) Data Release 2 (Tegmark et al. 2004), the SNe Ia data from Riess et al. (2004), and the H_0 prior from the *Hubble Space Telescope* (HST) Key Project with $H_0 = 72 \pm 8 \text{ km s}^{-1} \text{ Mpc}^{-1}$ (Freedman et al. 2001). The two models studied in Hannestad (2005) were also constrained in Wang et al. (2012) with updated cosmological data, where the

corresponding results turned out to be $\sum m_\nu < 0.627$ (95% CL) for an arbitrary (but constant) EoS and $\sum m_\nu < 0.476$ eV (95% CL) for the Λ CDM model. Based on the benefits of the more precise cosmological data, the bound on $\sum m_\nu$ is much more restrictive for each individual model, and the difference of the bounds on $\sum m_\nu$ from the two models is also reduced. The bound on $\sum m_\nu$ in the framework of time evolving EoS, $\omega(z) = \omega_0 + \omega_1 * z/(1+z)$, was also investigated in the literature (Xia et al. 2007, 2008; Li & Xia 2012), and revealed the degeneracy between $\sum m_\nu$ and the EoS ω parameters. In Smith et al. (2012), it was found that with non-vanishing curvature density parameter $\Omega_k \neq 0$ the 95% upper limit on $\sum m_\nu$ was more than double with respect to the case of a flat universe. This implies the strong degeneracy between curvature and $\sum m_\nu$.

In this paper, we present constraints on the total mass of ordinary (active) neutrinos $\sum m_\nu$ assuming no extra relics. Current cosmological data are not yet sensitive to the mass of individual neutrino species, i.e., the mass hierarchy. Under this situation, two scenarios for the mass splitting of the standard three-flavor neutrinos are often used in cosmology: (i) assuming three species of degenerate massive neutrinos, neglecting the small differences in mass expected from the observed mass splittings; and (ii) assuming the total neutrino mass dominated by the heaviest neutrino mass eigenstate (i.e., two massless and one massive neutrino). We will analyze and compare the constraints based on both the Λ CDM and ϕ CDM models in both the spatially flat ($\Omega_k = 0$) and non-flat ($\Omega_k \neq 0$) cases taking into account two different mass hierarchies. The ϕ CDM model—in which dark energy is modeled as a scalar field ϕ with a gradually decreasing (as a function of ϕ) potential $V(\phi)$ —is a simple dynamical model with dark energy density slowly decreasing in time. This model could resolve some of the puzzles of the Λ CDM model, such as the coincidence and fine-tuning problems (Peebles & Ratra 1988; Ratra & Peebles 1988). Here we focus on an inverse power-law potential $V(\phi) \propto \phi^{-\alpha}$, where α is a nonnegative constant (Peebles & Ratra 1988; Ratra & Peebles 1988). When $\alpha = 0$ the ϕ CDM model is reduced to the corresponding Λ CDM scenario. The ϕ CDM model with this kind of $V(\phi)$ has been extensively investigated, mostly in the spatially flat case (Podariu & Ratra 2000; Chae et al. 2004; Chen & Ratra 2004; Samushia et al. 2007; Samushia & Ratra 2010; Chen & Ratra 2011a, 2011b; Farooq & Ratra 2013; Farooq et al. 2013a, 2013b; Avsajanishvili et al. 2014; Pavlov et al. 2014; Chen et al. 2015; Lima et al. 2015), and only limited attention has been paid to the non-flat scenario (Pavlov et al. 2013; Farooq et al. 2015; Gosenca & Coles 2015). However, the above-mentioned literature on the ϕ CDM model did not consider massive neutrinos. In our previous work the ϕ CDM model with massive neutrinos has been studied under the assumption of spatial flatness (Chen & Xu 2016) using a combination of CMB data from *Planck* 2013 and other data sets. In this work, the ϕ CDM model with massive neutrinos will be further investigated in both flat and non-flat scenarios by using a combination of the CMB data from *Planck* 2015, BAO data from 6dFGS, SDSS-MGS, BOSS-LOWZ and CMASS-DR11, the joint light-curve analysis (JLA) compilation of SNe Ia observations, and two different H_0 priors.

The rest of the paper is organized as follows. Constraints from the cosmological data are derived in Section 2, and the results for the ϕ CDM model are compared with those for the

Λ CDM model in both the spatially flat and non-flat scenarios. We summarize our main conclusions in Section 3.

2. OBSERVATIONAL CONSTRAINTS

We consider four cosmological models with massive neutrinos in this paper, i.e., (i) the spatially flat Λ CDM model, (ii) the spatially non-flat Λ CDM model, (iii) the spatially flat ϕ CDM model, and (iv) the spatially non-flat ϕ CDM model. For each of the four models, we take into account two different scenarios for the neutrino mass hierarchy as mentioned above. Evolution of the background and perturbations are both considered within the linear perturbation theory. Appropriate formulae for the Λ CDM and ϕ CDM models in the spatially flat scenario are presented in Section 2 of Chen & Xu (2016). It is easy to generalize them to the non-flat scenario by inclusion of the curvature term Ω_k . The parameter spaces of the models under consideration are as follows:

$$\mathbf{P}_1 \equiv \{\Omega_b h^2, \Omega_c h^2, 100\theta_{\text{MC}}, \tau, \ln(10^{10} A_s), n_s, \sum m_\nu\}, \quad (1)$$

$$\mathbf{P}_2 \equiv \{\Omega_b h^2, \Omega_c h^2, 100\theta_{\text{MC}}, \tau, \ln(10^{10} A_s), n_s, \sum m_\nu, \Omega_k\}, \quad (2)$$

$$\mathbf{P}_3 \equiv \{\Omega_b h^2, \Omega_c h^2, 100\theta_{\text{MC}}, \tau, \ln(10^{10} A_s), n_s, \sum m_\nu, \alpha\}, \quad (3)$$

$$\mathbf{P}_4 \equiv \{\Omega_b h^2, \Omega_c h^2, 100\theta_{\text{MC}}, \tau, \ln(10^{10} A_s), n_s, \sum m_\nu, \alpha, \Omega_k\}, \quad (4)$$

where \mathbf{P}_1 and \mathbf{P}_2 are the parameter spaces of the Λ CDM model in the spatially flat and non-flat scenarios, respectively; \mathbf{P}_3 and \mathbf{P}_4 are the corresponding ones for ϕ CDM model in the flat and non-flat scenarios. Present-day densities of baryons and cold dark matter are denoted by $\Omega_b h^2$ and $\Omega_c h^2$, respectively, θ_{MC} is an approximation to the angular size of the sound horizon at the time of decoupling $\theta_* = r_s(z_*)/D_A(z_*)$ built in the CosmoMC package which is based on fitting formulae given in Hu & Sugiyama (1996), τ refers to the Thomson scattering optical depth due to reionization, n_s and A_s are the power-law index and amplitude of the power-law scalar primordial power spectrum of scalar perturbations, $\sum m_\nu$ is the sum of neutrino masses, Ω_k is the dimensionless spatial curvature density today, and α determines the steepness of the scalar field potential in the framework of ϕ CDM model.

2.1. Cosmological Data Sets

According to the constraints from the current cosmological observations the value of $\sum m_\nu \lesssim 1$ eV. This is below the limit to which the CMB power spectrum (excluding the late-time gravitational lensing effect on the power spectrum) alone can be sensitive (Komatsu et al. 2009). In other words, the massive neutrinos are relativistic at the decoupling epoch, so the effect of the massive neutrinos in the primary CMB power spectrum is very small. The main effect is around the first acoustic peak and is due to the early integrated Sachs–Wolfe effect. After the relativistic-to-non-relativistic transition, the massive neutrinos behave like cold matter. However, the non-relativistic massive neutrinos can suppress the CMB lensing potential on scales smaller than the horizon size. Thus CMB lensing is a useful probe for massive neutrinos. The CMB data set adopted here is a combination of the low multipoles ($l = 2\text{--}29$) joint TT, EE, BB and TE likelihood, and high multipoles joint TT ($l = 30\text{--}2508$), TE ($l = 30\text{--}1996$), and EE ($l = 30\text{--}1996$)

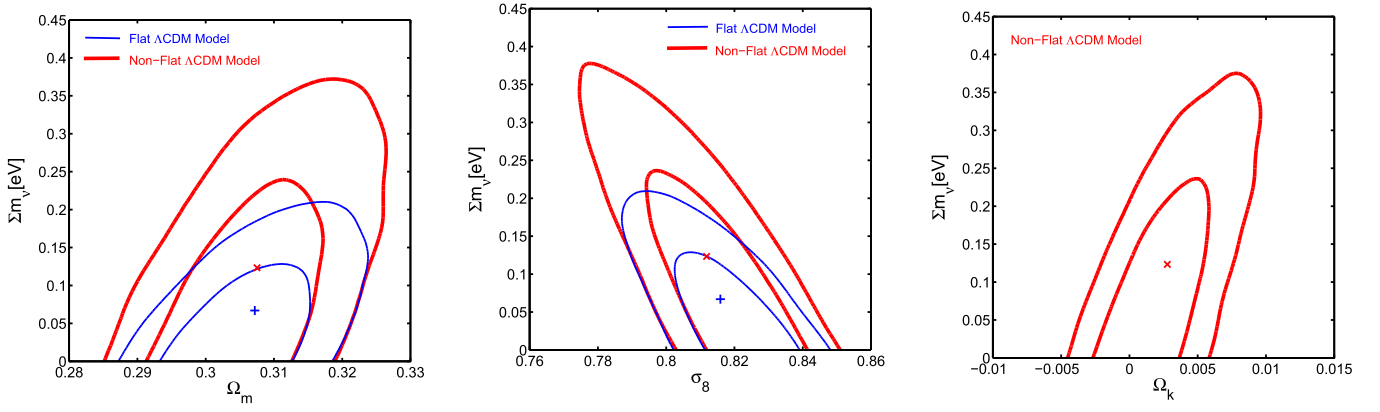


Figure 1. Contours refer to the marginalized likelihoods at 68% and 95% confidence levels constrained from the joint analysis using the *HST* H_0 prior for the Λ CDM model in the scenario assuming three species of degenerate massive neutrinos. Left and middle panels: contours in the $(\Omega_m, \Sigma m_\nu)$ and $(\sigma_8, \Sigma m_\nu)$ planes, where the thin blue (thick red) lines correspond to constraints in the flat (non-flat) scenario. The “+” (“x”) marks the mean values of the pair in the flat (non-flat) scenario. Right panel: contours in the $(\Omega_k, \Sigma m_\nu)$ plane for the non-flat scenario. The “x” marks the mean values of the $(\Omega_k, \Sigma m_\nu)$ pair.

likelihood, along with CMB lensing ($l = 40\text{--}400$) likelihood from *Planck* 2015 (Adam et al. 2015; Ade et al. 2015). BAO data from galaxy redshift surveys are a powerful cosmological probe, that can supply the Hubble expansion rate and angular diameter distance at different redshifts. The BAO data set employed here is a combination of measurements from the 6dFGS at $z_{\text{eff}} = 0.1$ (Beutler et al. 2011), the SDSS Main Galaxy Sample (MGS) at $z_{\text{eff}} = 0.15$ (Ross et al. 2014), the Baryon Oscillation Spectroscopic Survey (BOSS) “LOWZ” sample at $z_{\text{eff}} = 0.32$ and BOSS CMASS-DR11 anisotropic BAO measurements at $z_{\text{eff}} = 0.57$ (Anderson et al. 2014). Another important cosmological probe is offered by SNe Ia, which provided the first direct evidence for cosmic acceleration. The SNe Ia sample used here is the “JLA” compilation of SNe Ia (Betoule et al. 2014), which is a joint analysis of SNe Ia observations including several low-redshift samples ($z < 0.1$), all three seasons from the SDSS-II ($0.05 < z < 0.4$), three years from SNLS ($0.2 < z < 1$), and 14 very high redshift ($0.7 < z < 1.4$) from the *HST* observations. It totals 740 spectroscopically confirmed SNe Ia with high-quality light curves. The Riess et al. (2011) *HST* Cepheid + SNe Ia based estimate of $H_0 = (73.8 \pm 2.4) \text{ km s}^{-1} \text{ Mpc}^{-1}$ is also used as a supplementary “ H_0 -prior.” Another prior is the median statistics estimate of $H_0 = (68 \pm 2.8) \text{ km s}^{-1} \text{ Mpc}^{-1}$ of Chen & Ratra (2011), which is more consistent with H_0 values estimated using CMB and BAO data (e.g., Sievers et al. 2013; Aubourg et al. 2015; see also Calabrese et al. 2012).

2.2. Results and Analysis

In our analysis, the likelihood is assumed to be Gaussian, thus we have the total likelihood

$$\mathcal{L} \propto e^{-\chi_{\text{tot}}^2/2}, \quad (5)$$

where χ_{tot}^2 is constructed as

$$\chi_{\text{tot}}^2 = \chi_{\text{CMB}}^2 + \chi_{\text{BAO}}^2 + \chi_{\text{SNe}}^2 + \chi_{H_0}^2, \quad (6)$$

with χ_{CMB}^2 , χ_{BAO}^2 , χ_{SNe}^2 and $\chi_{H_0}^2$ denoting the contributions from CMB, BAO, SNe Ia and *HST* or median statistics H_0 prior data sets described above, respectively. We derive the posterior probability distributions of parameters with Markov Chain Monte Carlo (MCMC) exploration using the 2015 July version of CosmoMC (Lewis & Bridle 2002).

First, we give constraints assuming three species of degenerate massive neutrinos. Two-dimensional contours for the cosmological parameters of interest are shown in Figure 1 for the flat and non-flat Λ CDM models and in Figure 2 for the flat and non-flat ϕ CDM models. In these two figures the *HST* value of H_0 was assumed as a prior. One can see that constraints from the joint data sample are quite restrictive, though there are degeneracies between some parameters. Moreover, it turns out that with Ω_k as a free parameter the ranges of allowed values for other parameters (except $\Omega_b h^2$ and $100\theta_{\text{MC}}$) are all significantly broadened for both Λ CDM and ϕ CDM models.

In order to investigate the impact of the neutrino mass hierarchy, we compare the constraint results based on two different scenarios of the neutrino mass hierarchy as mentioned previously. Hereafter, the scenario of assuming three species of degenerate massive neutrinos will be quoted as “Scenario I” for short, and the scenario of assuming the total neutrino mass dominated by the heaviest neutrino mass eigenstate will be quoted as “Scenario II.” Corresponding mean values of the parameters of interest together with their 95% confidence limits constrained from the joint analysis using the *HST* H_0 prior are presented in Table 1 for the flat and non-flat Λ CDM models and in Table 2 for the flat and non-flat ϕ CDM models. It turns out that the constraints on $\Omega_b h^2$, $\Omega_c h^2$, $100\theta_{\text{MC}}$, τ , $\ln(10^{10} A_s)$, n_s , Ω_m , σ_8 and H_0 in the four models with different neutrino mass scenarios are consistent with each other at 95% CL. In the spatially flat case, we have $\Sigma m_\nu < 0.165(0.166) \text{ eV}$ at 95% CL in “Scenario I” (“Scenario II”) for the Λ CDM model, and $\Sigma m_\nu < 0.164(0.164) \text{ eV}$ at 95% CL in “Scenario I” (“Scenario II”) for the ϕ CDM model. In the spatially non-flat case, we have $\Sigma m_\nu < 0.299(0.354) \text{ eV}$ at 95% CL in “Scenario I” (“Scenario II”) for the Λ CDM model, and $\Sigma m_\nu < 0.301(0.364) \text{ eV}$ at 95% CL in “Scenario I” (“Scenario II”) for the ϕ CDM model. The results show that different neutrino mass scenarios just result in insignificant differences between the bounds on Σm_ν for both the Λ CDM and ϕ CDM models in the spatially flat case; however, in the spatially non-flat case, the corresponding differences are larger than those in the spatially flat case, and the allowed scale of Σm_ν in “Scenario II” is a little larger than that in “Scenario I.”

Let us focus on the constraints on Σm_ν and Ω_k . In “Scenario I,” the limits at 95% CL on the sum of neutrino

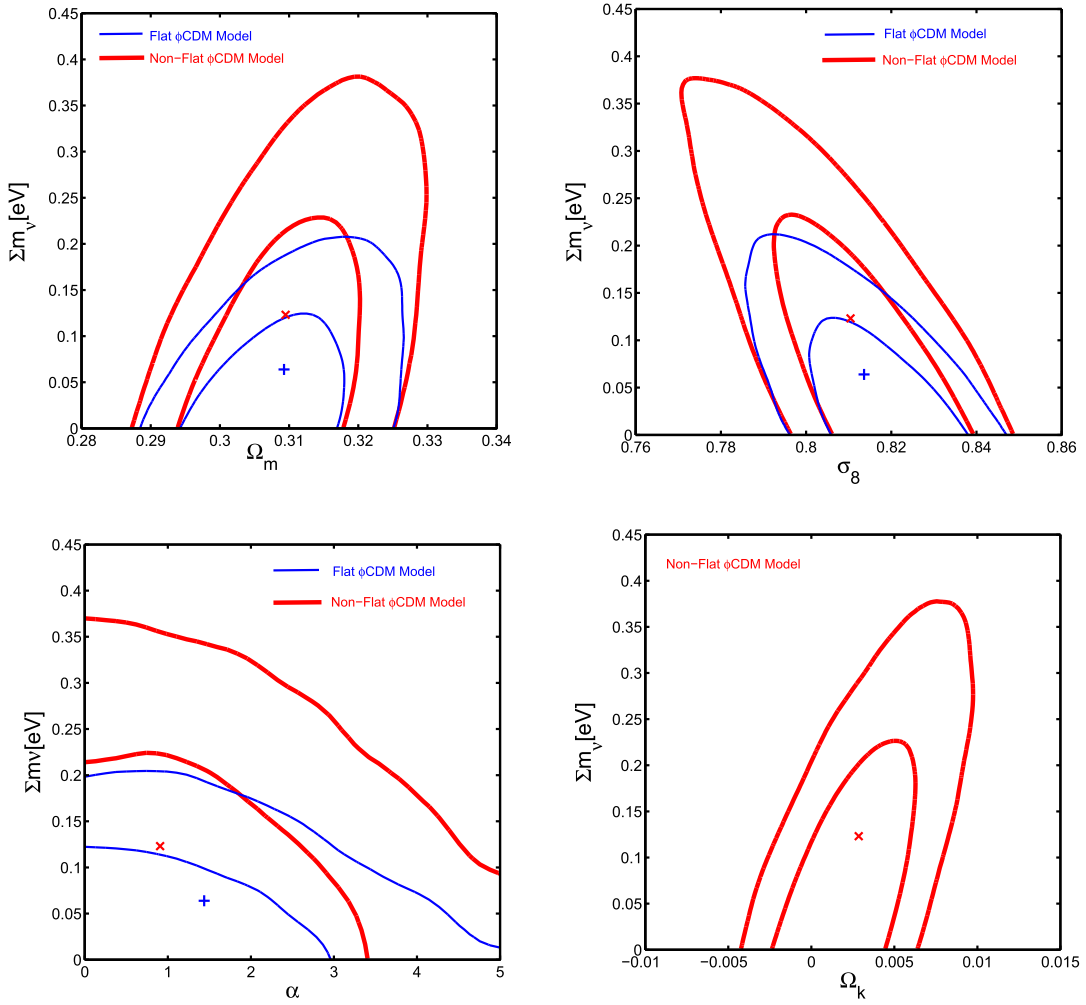


Figure 2. Contours refer to the marginalized likelihoods at 68% and 95% confidence levels constrained from the joint analysis using the *HST* H_0 prior for the ϕ CDM model in the scenario assuming three species of degenerate massive neutrinos. Upper left, upper right and lower left panels: contours in the $(\Omega_m, \Sigma m_\nu)$, $(\sigma_8, \Sigma m_\nu)$ and $(\alpha, \Sigma m_\nu)$ planes, where the thin blue (thick red) lines correspond to constraints in the flat (non-flat) scenario. The “+” (“x”) marks the mean values of the pair in the flat (non-flat) scenario. Lower right panel: contours in the $(\Omega_k, \Sigma m_\nu)$ plane for the non-flat scenario. The “x” marks the mean values of the $(\Omega_k, \Sigma m_\nu)$ pair.

Table 1
Constraints from the Joint Analysis Using the *HST* H_0 Prior, for the Λ CDM Model in Spatially Flat and Non-flat Cases with Two Different Scenarios for the Neutrino Mass Hierarchy

Parameters	Λ CDM model			
	Scenario I		Scenario II	
	Flat	Non-flat	Flat	Non-flat
$\Omega_b h^2$	0.0223 ± 0.0003	0.0222 ± 0.0003	0.0223 ± 0.0003	0.0222 ± 0.0003
$\Omega_c h^2$	0.1184 ± 0.0021	$0.1195^{+0.0030}_{-0.0029}$	0.1184 ± 0.0021	0.1196 ± 0.0030
$100\theta_{MC}$	1.0410 ± 0.0006	1.0408 ± 0.0006	1.0410 ± 0.0006	1.0408 ± 0.0006
τ	$0.0676^{+0.0289}_{-0.0260}$	$0.0715^{+0.0326}_{-0.0287}$	$0.0685^{+0.0279}_{-0.0260}$	$0.0739^{+0.0322}_{-0.0309}$
$\ln(10^{10} A_s)$	$3.0664^{+0.0537}_{-0.0488}$	$3.0767^{+0.0643}_{-0.0557}$	$3.0679^{+0.0520}_{-0.0486}$	$3.0812^{+0.0621}_{-0.0594}$
n_s	$0.9675^{+0.0082}_{-0.0080}$	0.9650 ± 0.0095	$0.9674^{+0.0079}_{-0.0078}$	$0.9642^{+0.0097}_{-0.0100}$
Ω_k	...	$0.0028^{+0.0055}_{-0.0051}$...	$0.0033^{+0.0058}_{-0.0051}$
Σm_ν (eV)	<0.165	<0.299	<0.166	<0.354
Ω_m	$0.307^{+0.014}_{-0.013}$	$0.308^{+0.016}_{-0.015}$	$0.308^{+0.014}_{-0.013}$	0.309 ± 0.016
σ_8	$0.816^{+0.022}_{-0.024}$	$0.812^{+0.028}_{-0.030}$	$0.815^{+0.023}_{-0.024}$	$0.807^{+0.032}_{-0.037}$
H_0 (km s $^{-1}$ Mpc $^{-1}$)	$67.87^{+1.05}_{-1.11}$	$68.22^{+1.43}_{-1.38}$	$67.83^{+1.03}_{-1.12}$	$68.18^{+1.36}_{-1.38}$

Note. “Scenario I” and “Scenario II” denote two different scenarios of the neutrino mass hierarchy, the implications of which are described in Section 2.2. We present the mean values with 95% confidence limits for the parameters of interest. The top block contains parameters with uniform priors that are varied in the MCMC chains. The lower block shows various derived parameters.

Table 2
Constraints from the Joint Analysis Using the *HST* H_0 Prior, for the ϕ CDM Model in Spatially Flat and Non-flat Cases with Two Different Scenarios for the Neutrino Mass Hierarchy

Parameters	ϕ CDM model			
	Scenario I		Scenario II	
	Flat	Non-flat	Flat	Non-flat
$\Omega_b h^2$	0.0223 ± 0.0003	0.0222 ± 0.0003	0.0223 ± 0.0003	0.0222 ± 0.0003
$\Omega_c h^2$	0.1183 ± 0.0021	0.1196 ± 0.0030	$0.1183^{+0.0021}_{-0.0022}$	0.1196 ± 0.0030
$100\theta_{MC}$	1.0410 ± 0.0006	1.0408 ± 0.0007	1.0410 ± 0.0006	1.0408 ± 0.0007
τ	$0.0685^{+0.0283}_{-0.0263}$	$0.0722^{+0.0330}_{-0.0313}$	$0.0699^{+0.0283}_{-0.0262}$	$0.0748^{+0.0319}_{-0.0298}$
$\ln(10^{10}A_s)$	$3.0679^{+0.0533}_{-0.0492}$	$3.0782^{+0.0642}_{-0.0601}$	$3.0703^{+0.0526}_{-0.0488}$	$3.0831^{+0.0616}_{-0.0567}$
n_s	$0.9680^{+0.0081}_{-0.0080}$	$0.9647^{+0.0096}_{-0.0092}$	$0.9678^{+0.0083}_{-0.0081}$	0.9643 ± 0.0097
Ω_k	...	$0.0031^{+0.0056}_{-0.0049}$...	$0.0036^{+0.0059}_{-0.0055}$
Σm_ν (eV)	<0.164	<0.301	<0.164	<0.364
α	<3.494	<3.938	<3.425	<3.941
Ω_m	0.309 ± 0.015	$0.311^{+0.017}_{-0.015}$	$0.310^{+0.015}_{-0.014}$	0.311 ± 0.017
σ_8	$0.814^{+0.023}_{-0.024}$	$0.809^{+0.028}_{-0.031}$	$0.813^{+0.023}_{-0.025}$	$0.805^{+0.033}_{-0.038}$
H_0 ($\text{km s}^{-1} \text{Mpc}^{-1}$)	$67.61^{+1.24}_{-1.34}$	$67.89^{+1.49}_{-1.50}$	$67.57^{+1.20}_{-1.33}$	$67.91^{+1.45}_{-1.50}$

Note. The mean values with 95% confidence limits for the parameters of interest are displayed. The top block contains parameters with uniform priors that are varied in the MCMC chains. The lower block shows various derived parameters. The implications of “Scenario I” and “Scenario II” are the same as those in Table 1.

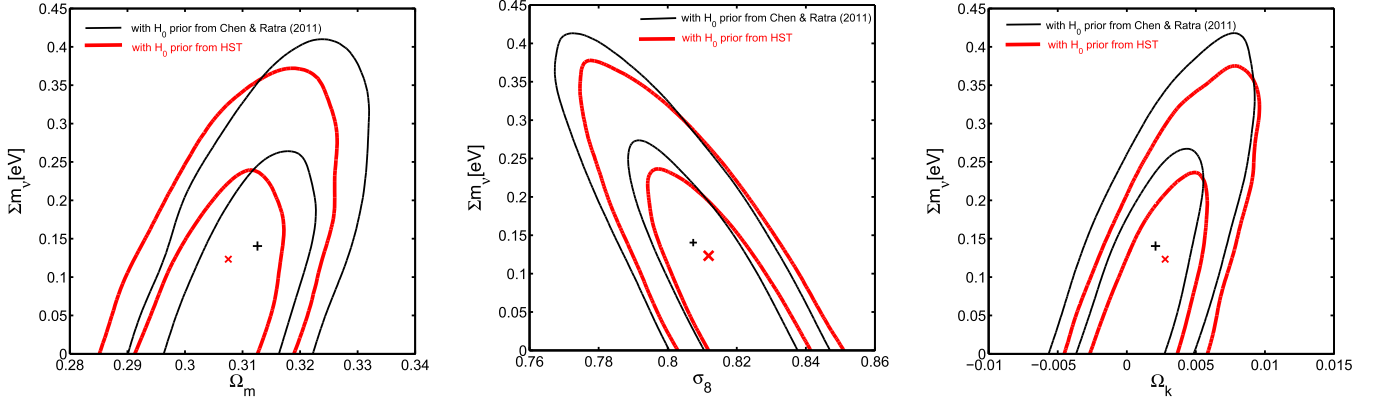


Figure 3. Contours refer to the marginalized likelihoods at 68% and 95% confidence levels in the non-flat Λ CDM model assuming three species of degenerate massive neutrinos constrained from the joint sample with two different H_0 priors. From left to right, contours in the $(\Omega_m, \Sigma m_\nu)$, $(\sigma_8, \Sigma m_\nu)$ and $(\Omega_k, \Sigma m_\nu)$ planes are presented, respectively. The thin black lines correspond to constraints from the joint sample with the $H_0 = (68 \pm 2.8) \text{ km s}^{-1} \text{ Mpc}^{-1}$ prior from Chen & Ratra (2011). The thick red lines correspond to constraints from the joint sample with the $H_0 = (73.8 \pm 2.4) \text{ km s}^{-1} \text{ Mpc}^{-1}$ (Riess et al. 2011) prior from *HST* observations. The “+” marks the mean values of the corresponding pair with H_0 prior from Chen & Ratra (2011). The “x” marks the mean values with H_0 prior from Riess et al. (2011).

masses are $\Sigma m_\nu < 0.165(0.299) \text{ eV}$ for the flat (non-flat) Λ CDM model, and $\Sigma m_\nu < 0.164(0.301) \text{ eV}$ for the flat (non-flat) ϕ CDM model. It shows that with Ω_k as a free parameter the 95% upper limit on Σm_ν is about double that in the flat case for both the Λ CDM and ϕ CDM models. One can obtain the same conclusion in “Scenario II.” The strong correlation between Ω_k and Σm_ν is because that the massive neutrinos are still relativistic until recombination so they act as an additional radiative component, and the constraint results also demonstrate that the spatially flat universe is still highly preferred.

In order to explore the impact of the prior value of the Hubble constant H_0 on the cosmological parameter estimation, we compare the constraints resulting from the joint data sample with two different H_0 priors in the non-flat Λ CDM model assuming three species of degenerate massive neutrinos. One is from *HST* observation with $H_0 = (73.8 \pm 2.4) \text{ km s}^{-1} \text{ Mpc}^{-1}$ (Riess et al. 2011) which is used above, and another is from the median statistics analysis of Chen & Ratra (2011) with $H_0 = (68 \pm 2.8) \text{ km s}^{-1} \text{ Mpc}^{-1}$. Two-dimensional confidence

contours for the cosmological parameters of interest are shown in Figure 3 for the non-flat Λ CDM model with the two different H_0 priors. One can see that the prior value of the Hubble constant H_0 affects cosmological parameter estimation, but not very significantly. In our combined analysis it is because of the weight of the other data used. However, one can notice a certain trend, namely with smaller values of the H_0 prior, the upper limit on Σm_ν gets larger. This implies that the parameters H_0 and Σm_ν are negatively correlated (Komatsu et al. 2009; Chen & Xu 2016). Our result is consistent with that of Di Valentino et al. (2016) who conclude that the bounds on the neutrino parameters may differ appreciably depending on the prior values of low redshift quantities, such as the Hubble constant, the cluster mass bias, and the reionization optical depth.

3. CONCLUSION

We have studied the Λ CDM and ϕ CDM models with massive neutrinos assuming two different neutrino mass

hierarchies in both the spatially flat and non-flat scenarios. In the ϕ CDM model under consideration, the dark energy scalar field ϕ with an inverse power-law potential $V(\phi) \propto \phi^{-\alpha}$ ($\alpha > 0$) powers the late-time accelerated cosmological expansion. In order to constrain model parameters, we performed a joint analysis on the data including *Planck* 2015 data comprising temperature and polarization of CMB anisotropies as well as CMB lensing, BAO data from 6dFGS, SDSS-MGS, BOSS-LOWZ and CMASS-DR11, the JLA compilation of SNe Ia observations, and the H_0 prior according to *HST* or median statistics. The results indicate that constraints on the cosmological parameters from this combination of data are quite restrictive. We find that the constraints on the parameters are much tighter than those in the previous literature (Chen & Xu 2016), which made use of a combination of the CMB temperature power spectrum likelihoods from *Planck* 2013 and the CMB polarization power spectrum likelihoods from nine-year *WMAP* (*WMAP9*), the galaxy clustering data from WiggleZ and BOSS DR11, and the JLA compilation of SNe Ia observations. A more recent paper by Chen & Xu (2016) studying the Λ CDM and ϕ CDM models with massive neutrinos assumed only the spatially flat case.

The results of our paper clearly show that cosmological bounds on the total neutrino mass Σm_ν are very tight; however, they are significantly correlated with the curvature term. It turns out that with Ω_k as a free parameter the 95% upper limit on Σm_ν is relaxed by more than a factor of two with respect to that in the flat case for both the Λ CDM and ϕ CDM scenarios. Furthermore, the bounds on Σm_ν based on two different neutrino mass hierarchies have insignificant differences in the spatially flat case for both the Λ CDM and ϕ CDM models; however, the corresponding differences are larger in the non-flat case. Moreover, for a given neutrino mass hierarchy, the bounds on Σm_ν in Λ CDM and ϕ CDM scenarios have small differences, irrespective of whether Ω_k is fixed at zero or is taken as a free parameter. For example, in the scenario of assuming three species of degenerate massive neutrinos, when $\Omega_k = 0$, we have $\Sigma m_\nu < 0.165(0.164)$ eV at 95% CL for the Λ CDM (ϕ CDM) model; when $\Omega_k \neq 0$, we have $\Sigma m_\nu < 0.299(0.301)$ eV at 95% CL for the Λ CDM (ϕ CDM) model. Additionally, in the scenario assuming three species of degenerate massive neutrinos, we find $\alpha < 3.494(3.938)$ at 95% CL for the flat (non-flat) ϕ CDM model, while the Λ CDM scenario corresponding to $\alpha = 0$ is not ruled out at this CL. One can obtain the same conclusion in the scenario assuming the total neutrino mass dominated by the heaviest neutrino mass eigenstate. In general, the constraints on the cosmological parameters are similar in the Λ CDM and ϕ CDM models, and the bounds on the total neutrino mass Σm_ν are not particularly sensitive to the underlying cosmological models under consideration. Massive neutrinos mainly affect the redshift of matter–radiation equality z_{eq} (and also being relativistic at the z_{eq} they are counted as non-relativistic now, thus being entangled with $\Omega_c h^2$). At this epoch neither Λ nor ϕ contributes significantly to the background expansion. Consequently, these results imply that the observational data that we have employed here still cannot distinguish whether dark energy is a time-independent cosmological constant or varies mildly in space and slowly in time.

Y.C. would like to thank Jun-Qing Xia for useful discussions. Y.C. was supported by the National Natural

Science Foundation of China (Nos. 11133003 and 11573031), the China Postdoctoral Science Foundation (No. 2015M571126), and the Young Researcher Grant of National Astronomical Observatories, Chinese Academy of Sciences. B.R. was supported in part by DOE grant DEFG 03-99EP41093. M.B. was supported by the Polish NCN grant DEC-2013/08/M/ST9/00664 and the Poland-China Scientific and Technological Cooperation Committee Project No. 35-4. M.B. obtained approval of a foreign talent introducing project in China and gained special fund support of a foreign knowledge introducing project. S.L. was supported by the National Natural Science Foundation of China under grants No. 11347163 and the Science and Technology Program Foundation of the Beijing Municipal Commission of Education of China under grant No. KM201410028003. Z.H.Z. was supported by the Chinese Ministry of Science and Technology National Basic Science Program (Project 973) under grant Nos. 2012CB821804 and 2014CB845806. Y.C. and Z.H.Z. were also supported by the Strategic Priority Research Program “The Emergence of Cosmological Structure” of the Chinese Academy of Sciences (No. XDB09000000).

REFERENCES

- Abe, S., et al. KamLAND Collaboration 2008, *PhRvL*, **100**, 221803
 Adam, R., et al. Planck Collaboration arXiv:1502.01582
 Ade, P. A. R., et al. Planck Collaboration arXiv:1502.01589
 Agafonova, N., et al. OPERA Collaboration 2010, *PhLB*, **691**, 138
 Ahmad, Q. R., et al. SNO Collaboration 2001, *PhRvL*, **87**, 071301
 Ahn, J. K., et al. RENO collaboration 2012, *PhRvL*, **108**, 191802
 An, F. P., et al. Daya Bay Collaboration 2012, *PhRvL*, **108**, 171803
 Anderson, L., Aubourg, É, Bailey, S., et al. 2014, *MNRAS*, **441**, 24
 Ashie, Y., et al. Super-Kamiokande Collaboration 2005, *PhRvD*, **71**, 112005
 Aubourg, E., Bailey, S., Bautista, J. E., et al. 2015, *PhRvD*, **92**, 123516
 Avsajanishvili, O., Arkipova, N. A., Samushia, L., & Kahnishvili, T. 2014, *EPJC*, **74**, 3127
 Avsajanishvili, O., Samushia, L., Arkipova, N. A., & Kahnishvili, T. 2015, arXiv:1511.09317
 Balantekin, A. B., & Haxton, W. C. 2013, *PrPNP*, **71**, 150
 Bennett, C. L., Halpern, M., Hinshaw, G., et al. 2003, *ApJS*, **148**, 1
 Betoule, M., Kessler, R., Guy, J., et al. 2014, *A&A*, **568**, A22
 Beutler, F., Blake, C., Colless, M., et al. 2011, *MNRAS*, **416**, 3017
 Calabrese, E., Archidiacono, M., Melchiorri, A., & Ratra, B. 2012, *PhRvD*, **86**, 043520
 Chae, K.-H., Chen, G., Ratra, B., & Lee, D.-W. 2004, *ApJL*, **607**, L71
 Chen, G., & Ratra, B. 2004, *ApJL*, **612**, L1
 Chen, G., & Ratra, B. 2011a, *PASP*, **123**, 1127
 Chen, Y., & Ratra, B. 2011b, *PhLB*, **703**, 406
 Chen, Y., & Xu, L. 2016, *PhLB*, **752**, 66
 Chen, Y., Geng, C.-Q., Cao, S., Huang, Y.-M., & Zhu, Z.-H. 2015, *JCAP*, **02**, 010
 Di Valentino, E., Giusarma, E., Mena, O., Melchiorri, A., & Silk, J. 2016, *PhRvD*, **93**, 083527
 Farooq, O., Crandall, S., & Ratra, B. 2013a, *PhLB*, **726**, 72
 Farooq, O., Mania, D., & Ratra, B. 2013b, *ApJ*, **764**, 138
 Farooq, O., Mania, D., & Ratra, B. 2015, *ApSS*, **357**, 11
 Farooq, O., & Ratra, B. 2013, *ApJL*, **766**, L7
 Fogli, G. L., Lisi, E., Marrone, A., & Palazzo, A. 2006, *PrPNP*, **57**, 742
 Freedman, W. L., Madore, B. F., Gibson, B. K., et al. 2001, *ApJ*, **553**, 47
 Fukuda, Y., et al. Super-Kamiokande Collaboration 1998, *PhRvL*, **81**, 1562
 Gosenca, M., & Coles, P. 2015, arXiv:1502.04020
 Hannestad, S. 2005, *PhRvL*, **95**, 221301
 Hu, W., & Sugiyama, N. 1996, *ApJ*, **471**, 542
 Komatsu, E., Dunkley, J., Nolte, M. R., et al. 2009, *ApJS*, **180**, 330
 Lesgourgues, J., & Pastor, S. 2006, *PhR*, **429**, 307
 Lesgourgues, J., & Pastor, S. 2012, *AdHEP*, **2012**, 608515
 Lewis, A., & Bridle, S. 2002, *PhRvD*, **66**, 103511
 Li, H., & Xia, J.-Q. 2012, *JCAP*, **11**, 039
 Lima, N. A., Liddle, A. R., Sahlén, M., & Parkinson, D. 2015, arXiv:1501.02678
 Maltoni, M., Schwetz, T., Tortola, M. A., & Valle, J. W. F. 2004, *NJPh*, **6**, 122

- Pavlov, A., Farooq, O., & Ratra, B. 2014, [PhRvD](#), **90**, 023006
- Pavlov, A., Westmoreland, S., Saaidi, K., & Ratra, B. 2013, [PhRvD](#), **88**, 123513
- Peebles, P. J. E., & Ratra, B. 1988, [ApJL](#), **325**, L17
- Podariu, S., & Ratra, B. 2000, [ApJ](#), **532**, 109
- Ratra, B., & Peebles, P. J. E. 1988, [PhRvD](#), **37**, 3406
- Riess, A. G., Macri, L., Casertano, S., et al. 2011, [ApJ](#), **730**, 119
- Riess, A. G., Strolger, L.-G., Tonry, J., et al. 2004, [ApJ](#), **607**, 665
- Ross, A. J., Samushia, L., Howlett, C., et al. 2014, arXiv:1409.3242
- Samushia, L., Chen, G., & Ratra, B. 2007, arXiv:0706.1963
- Samushia, L., & Ratra, B. 2010, [ApJ](#), **714**, 1347
- Sievers, J. L., Hlozek, R. A., Nolta, M. R., et al. 2013, [JCAP](#), **1310**, 060
- Smith, A., Archidiacono, M., Cooray, A., et al. 2012, [PhRvD](#), **85**, 123521
- Tegmark, M., Strauss, M. A., Blanton, M. R., et al. 2004, [PhRvD](#), **69**, 103501
- Wang, X., Meng, X.-L., Zhang, T.-J., et al. 2012, [JCAP](#), **11**, 018
- Xia, J.-Q., Li, H., Zhao, G.-B., & Zhang, X. 2008, [PhRvD](#), **78**, 083524
- Xia, J.-Q., Zhao, G.-B., & Zhang, X. 2007, [PhRvD](#), **75**, 103505